

An IoT-based Framework to Forecast Indoor Air Quality using ANFIS-DTMC Model

Krati Rastogi

and

Divya Lohani

Department of Computer Science & Engineering, Shiv Nadar University, Gautam Buddha Nagar, Uttar Pradesh, India

As humans spend around 90% of their time indoors, Indoor Air Quality (IAQ) is a subject of major concern for the physical and mental well-being of humans. According to the United States Environment Protection Agency (US EPA), even in centrally air-conditioned buildings, indoor air is much more polluted than outdoor air, mainly due to changes in occupancy patterns, old or ill-maintained ventilation systems and dust. Therefore, it becomes important to measure and analyze IAQ. In this work, an end to end IoT system has been developed to sense and analyze indoor environmental parameters: Temperature (T), relative humidity (RH), carbon dioxide (CO_2), carbon monoxide (CO), particulate matter (PM_{10} and $PM_{2.5}$). For analysis purpose, a new index, namely, State of Indoor Air (SIA) has been proposed using adaptive neuro-fuzzy inference system (ANFIS). ANFIS model serves as a basis for constructing a set of fuzzy rules, to generate a specified pair of input-output with appropriate membership functions. SIA categorizes the state of indoor air as satisfactory, moderate or poor. Finally, a DTMC model has been used to forecast the change in SIA states by generating transition matrix and computing return periods of each SIA state. The accuracy of the proposed model is found to be satisfactory with a low average absolute prediction error of 2.60%.

Keywords: Internet of Things, Indoor Air Quality, Ventilation Rate, Thermal Comfort, Air Change Rate, Air Quality Index, Adaptive Neuro-Fuzzy Inference System, Discrete Time Markov Chain.

1. INTRODUCTION

Good air quality is critical to healthy and productive life in the indoor environment. People spend around 90 percent of the time in an indoor environment (Kim et al., 2014), which these days are mostly heating, ventilation and air conditioning (HVAC) controlled. An indoor environment is a combination of thermal, mechanical/non mechanical, electronics, atmospheric, psychological and various other types of factors (United States Environment Protection Agency, 2018). Recently, the health effects of indoor air pollution have received attention because of the dominant exposure of indoor air pollutants to people, who spend a significant portion of time in the indoor environment (Kim et al., 2014), which these days are mostly tightly insulated and concentrated with pollutants. These pollutants have hazardous health issues as Sick Building Syndrome (SBS) and Building Related Illness (BRI). Sickness and discomfort experienced by the occupants due to the Indoor Air Quality (IAQ) is related as SBS and BRI. Poor air quality may have a much adverse effect on the younger generation especially those residing in University premises. Most of the students time is spent indoors, and in an air-conditioned environment, where there is a limited scope of fresh air circulation (Johansson et al., 2014) it is imperative to monitor the indoor air quality. These gases are toxic in nature (Ko et al., 2008) and it may be one of the reasons for various illnesses in students resulting in poor concentration, irregular attendance in class and poor academic performance. Pollutants have harmful effects on the skin and eyes, and allergies on a different part of the human body. The high pollutant concentration is due various factors such as irregular air circulation and ventilation system, gas leaks, burning, decomposition of material, tobacco sources, insulating materials such as newly installed carpets, floorings or plasters, furniture products, pesticides, products for household cleaning and heating/humidification devices (Ko et

al., 2008). Appropriate ventilation is essential to decrease indoor pollutants and make indoor air quality suitable for human health and comfort. Air quality has an index that represents the quality of air. CO_2 is one of the gases which is always present in indoor environment. CO_2 is one of the highest elements in the indoor environment due to respiration and activities in an enclosed space decreased oxygen level and increased CO_2 level. For carbon dioxide American Society of Heating, Refrigerating, and Air-Conditioning Engineers (ASHRAE) maximum 1000 PPM in the room in an indoor room (ASHRAE/ANSI Standard 62.1, (2013)). When the exchange of air is processed during ventilation outdoor PM is introduced in the indoor environment. Human movement to and from the rooms introduces polluted outdoor air inside the rooms, which is another cause of the presence of outdoor PM in the indoor environment. The environmental factors that influence the thermal comfort of indoor occupants are metabolic rate, clothing level, air temperature, mean radiant temperature, air speed, and humidity. An increase in indoor temperature and humidity leads to growth of microbial contaminants (mold, fungus). Major sources of indoor carbon monoxide (CO) are combustion due to smoking, cooking, heating or incense burning. It is also introduced by infiltration of outdoor air into indoor environment (Spachos and Hatzinakos, 2016). Exposure to high concentrations of CO causes dizziness, headaches, reduced brain function and impaired vision and coordination.

Contribution of this work: With the introduction of wireless air quality sensors that can pair with most contemporary smartphones, it is now possible to monitor indoor environment pervasively in real time, take precautionary measures, and maintain a healthy life. This work aims to develop an IoT-based system monitor indoor air quality parameters in real time; and proposes a new indoor air quality index (named as SIA) which determines the state of indoor air based on the concentrations of various indoor air parameters - temperature (T), relative humidity (RH), carbon dioxide (CO_2), carbon monoxide (CO) and particulate matter ($PM_{2.5}$ and PM_{10}). The values of six indoor parameters are used to compute thermal comfort, ventilation rate and indoor air quality index (AQI). Thermal comfort is represented by the percent of dissatisfied people (PPD), ventilation rate (VR) is estimated using air change rate (ACH) from CO_2 concentration and AQI is obtained from CO, $PM_{2.5}$ and PM_{10} concentrations. The PPD, VR and AQI obtained are fed to an adaptive neuro-fuzzy inference system (ANFIS) to determine the current state of IAQ and the proportion of time for which the air quality of the classroom is not healthy. The indoor occupants are interested in the proportion of time for which the IAQ stays in a particular SIA state and the time after which an undesirable SIA will occur again. Therefore, the work also forecasts the future SIA based on the current state, using Discrete Time Markov Chain (DTMC) model. The prediction performance of the proposed parameter has been evaluated using real time data. The predicted return periods are validated against actual return periods of SIA for the testing period. The working of the proposed system is explained with the help of the flowchart in Figure 1. This work introduces a novel approach to designating the status of indoor air using multiple indoor pollutants as well as environmental parameters. The proposed index takes all possible factors of human health and comfort into consideration in classifying the state of indoor environment as poor, moderate or satisfactory. To the best of authors knowledge, no other works have taken the three factors, i.e. pollutant concentration, thermal comfort and ventilation into contemplation in determining the state of indoor air.

The rest of the paper is organized as follows: Section 2 presents the state of art literature review of works dealing with IAQ. Section 3 describes our IoT-based system for sensing, visualization, and analysis. Section 4 describes the calculations for PPD, ventilation rate and indoor AQI. It also discusses the ANFIS model and how SIA of a classroom is calculated. Sections 5 discusses the development of DTMC model to forecast the SIA index, Section 6 presents a comparison between the predicted values and actual data. Section 6 concludes the paper.

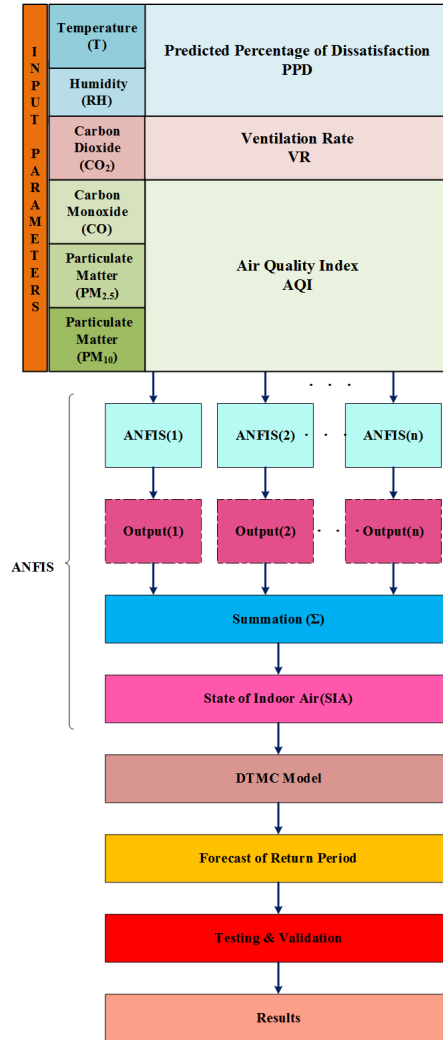


Fig 1: Flow chart explaining the functioning of the proposed system

2. LITERATURE REVIEW

This section describes the research work related to the use of fuzzy inference, artificial neural networks and IoT in IAQ and thermal comfort monitoring systems. Works related to monitoring and analysis of IAQ with the help of wireless and IoT based systems are discussed first. An air quality monitoring system is presented in (Bhattacharya et al., 2012) to create a smart home environment. It uses environmental parameters such as temperature, humidity, gaseous emissions and aerosol / particulate matter, to assess the health of an indoor space. It also presents controlling of HVAC (Heating, Ventilation and Air Conditioning) with Air Quality Index and environmental parameters as input reflects that in terms of the Air Quality Index (AQI) and offers environmental information as feedback to monitor the HVAC system (heating, ventilation and air conditioning) in a smart house. Kim et al. (2014) developed a real-time system to monitor and timely alert about indoor air quality. Author looks at the complexities of designing and implementing an integrated sensing network for real-time indoor air quality monitoring, facilities, information processing, and. The device aims to detect on a real-time basis the level of seven pollutants, ozone (O_3), particulate matter, carbon monoxide (CO), nitrogen oxides (NO_2), sulfur dioxide (SO_2), volatile organic compound, and carbon dioxide (CO_2), and provides timely

notification of the overall air quality.

A self-developed server program (Saad et al. 2013) which explain the flow of data from base station to the server as gaseous pollutants as parameters to build web-based system. It also explains the physical factors that affect the indoor air quality and their effects. Yu et al. (2013) built an indoor air quality monitoring system which reduces the error percentage from 15% to 7%. System functions use calibration method to strength the measurement value's sensitivity and accuracy.

Association between SBS and IAQ is investigated by a few authors. The importance predictors of sick building syndromes are ventilation and accumulation of possible contaminants within the indoor environment (Norhidayah et al., 2013). Effect of temperature and humidity on thermal comfort and IAQ is discussed in some research works. A system (Fang et al., 1998) is designed with various combinations of temperature and humidity in the 18-28 °C and 30-70 percent RH ranges. A specially designed test system was built and a series of experiments was planned to independently observe the effect of temperature and humidity on air quality / odor intensity perception and pollutant emission from the products. With different combinations of ranges of humidity and temperature and found to be linearly correlated. The air was perceived as less acceptable with increasing temperature and humidity. Stazi et al. (2017) developed an automatic system for window openings, based on both thermal comfort and indoor air quality correlations. The authors concluded that the stronger driving force for window opening is thermal comfort, while the improvement of air quality is a secondary constraint. Mei et al. (2017) present a direct expansion (DE) air conditioning (A/C) system which not only improves indoor air quality and thermal comfort but also reduces the energy consumption. The advantages of the proposed energy-optimized system are verified by simulation results.

Mendes et al. (2015) explored buildings characteristics and environmental variables in 22 elderly care centers in Portugal. Indoor environmental parameters and thermal comfort (TC) parameters were measured to determine concentrations of PM_{10} , $PM_{2.5}$, TVOC, bacteria, CO, CO_2 , predicted mean vote (PMV) and predicted the percent of dissatisfied people (PPD) indices. To assess the impact of energy upgrades on indoor air quality and occupant comfort, concentrations of indoor air pollutants and thermal parameters such as temperature and relative humidity were measured in 15 dwellings before and after the energy upgrade in (Broderick et al., 2017). It was observed that although energy retrofit had a positive impact on occupant comfort and building temperature, concentrations of some pollutants were found to increase following the retrofit.

Al horr. et al. (2016) presented the state of the art study of indoor environmental quality (IEQ) and its effect on the well-being and comfort of occupants. An extensive review of the literature has been provided to establish links between IEQs and occupant well-being and comfort. Important associated issues like indoor air quality thermal comfort, visual comfort, acoustic comfort, and sick building syndrome are considered. Thermal comfort, perceived air quality, sick building syndrome symptoms, and cognitive performance were tested in an office in Singapore on 56 acclimatized persons (Schiavon et al., 2017), exposed for 90 minutes to each of five conditions: 23, 26, and 29C, and in the latter 2 cases, with and without occupantcontrolled air movement. The best cognitive performance (as indicated by task speed) was obtained at 26C and the worst at 23.

Fuzzy systems have been used for determination and control of IAQ. Meana-Llorin and Garca (2017), have detailed the design, implementation, and testing of an IoT based fuzzy inference system, which is able to recognize the fall of a human being in an accurate manner. The fuzzy inference system fuses data from multiple sensors to infer that a fall has occurred. Moulik and Majumdar (2019) presented an approach to control the indoor temperature using the Internet of Things platform and fuzzy logic in order to set a more comfortable environment for their users. The authors claim that the fuzzy approach helped achieve an energy saving of around 40%. Kumar et al. (2018) proposed a Cloud and IoT based mobile healthcare application which uses a classification algorithm called Fuzzy Rule based Neural Classifier for diagnosis and severity

estimation of diabetes. Experimental results indicate that the proposed work outperforms the existing systems for disease prediction.

Kaur J. and Kaur K. (2017) proposed a framework that uses fuzzy inference to perform automatic employee performance appraisal on the basis of data sensed from IoT. Raw IoT data is classified into three activities, positive, negative and neutral. The framework co-locates employee and corresponding activity so as to calculate employee implication and then uses fuzzy logic to perform cognitive decision making. Ajeev et al. (2015) used fuzzy logical inference to detect traffic anomaly in an IoT network. Modified stochastic approximation and sliding window are suggested for traffic anomaly detection. The results of experimental assessment of the proposed techniques are discussed.

In all these works, one or other aspects of indoor environment have been investigated. The literature lacks research works which provide a complete solution to address all the three aspects of indoor environment: air quality, thermal comfort and ventilation. This work attempts to build a system which taken into consideration all the factors that affect the indoor environment.

3. IOT SYSTEM ARCHITECTURE

3.1 IoT Sensing Setup

A sensing architecture of an enormous amount of real-time generation of indoor air pollutants is shown in Figure 2, consists of an IoT setup for continuous monitoring, collection, storage, analysis, visualization of real time data. IoT cloud service is used for storage, analysis and visualization of pollutant concentrations. The sensed indoor air pollutant concentrations are collected by Arduino Uno and transmitted to a smartphone application. It uses Arduino Uno, which is an ATmega328P 8-bit micro-controller, has 14 digital input/output pins, 6 analog input pins, a power jack, a USB connection, a 16 MHz quartz crystal, an ICSP header and a reset button. The sensors used for measuring the environmental parameters are wired to Arduino. A constant source of power supply instead of batteries is used to the system as the setup is fixed for the classroom. DHT-22 sensor collects information about temperature and humidity whose V_{cc} pin is connected to 5V pin of Arduino, GND pin is connected to ground pin of Arduino, output pin is connected to Digital Pin 2 of Arduino. Whereas gas sensor MQ135 that detects CO_2 levels inside the room with V_{cc} pin of MQ135 is connected to 5V pin of Arduino, GND pin is connected to the ground pin of Arduino, output pin is connected to Analog Pin 0 of Arduino.

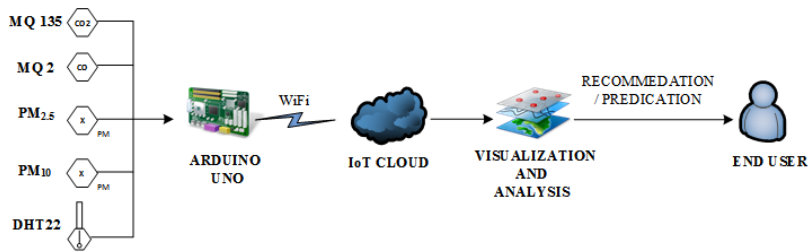


Fig. 2: Our IoT Sensing System

In order to standardize the CO_2 values; we have used an off-the-shelf sensor Sensordrone, which can directly transmit data to an Android Application over Bluetooth. Sensordrone contains 11 on-board sensors and has an option of using various sensor modules as the attachment. Optical sensor PPD42NS with dimensions 59mm 45mm 22 mm measures the PM level in air by recording the low pulse occupancy (LPO) time. It is sensitive to particulates of diameter up to 1 μ m. Analog pin is connected to pin 3 of Arduino, V_{cc} to 5V pin, ground to ground of Arduino. It has been used to collect $PM_{2.5}$ and PM_{10} concentrations. Additionally, an off-the-shelf sensor Air

Visual Air Quality Monitor is used to standardize the indoor $PM_{2.5}$ and PM_{10} values, which can directly transmit data to an Android Application over WiFi. MQ2 sensor is used to measure CO concentration in the room. With the pin configuration of Arduino V_{cc} pin of MQ2 is connected to 5V pin, GND pin is connected to ground pin of Arduino, O/P pin is connected to Analog Pin 1 of Arduino. MQ sensors have fast response time and high sensitivity but these sensors must be calibrated before actual measurements.

Arduino Uno uses Wifi module ESP 8266 for communicating/sending the measurements of ambient temperature (in degree Celsius), relative humidity (in percentage) and CO_2 concentration (in ppm), $PM_{2.5}$ and PM_{10} (in g/m^3) values to the IoT cloud, where it is stored for visualization, analysis and forecasting. Additionally, as the whole campus is WiFi-enabled, therefore, ESP8266 is connected to Arduino board as follows: V_{cc} pin is connected to 3.3V of Arduino, GND pin is connected ground pin of Arduino, TX goes to RX pin of Arduino, RX is connected to TX pin of Arduino, chip enable is connected to 3.3V of Arduino, GPIO0 and GPIO2 are general purpose pins. RST pin to reset the chip.

Amazon Web Services (AWS) is used for storage, processing, analysis and visualization of a large amount of data using. AWS IoT is a cloud-managed platform that lets connected devices communicate with cloud applications and other devices easily and securely. AWS IoT can support trillions of devices and trillions of messages, and can reliably and securely process and route those messages to AWS endpoints and other devices. With broad and deep platform, Amazon Web Services provides users with the highest level of security they need. To access the data, the user will get the account ID and password. By offering certificates, public and private keys, the AWS helps connect the board to the particular account through Wi-Fi.

3.1.1 Test Bed and IoT Setup Placement .: For this study, the classroom of Engineering block in the university, equipped with centralized heating, ventilation and air conditioning (HVAC) systems are chosen. The room under observation has 49.5139.50 feet floor plan and 9.58 feet high ceiling. The classroom consists of two windows and two doors, all of which are fully sealed during the experiment. The IoT setup is mounted in such a way that it is not exposed directly to sunlight, heat and human breathing. The setup is placed 6 feet away from door/windows and at least 2 feet above the floor, in such a manner that there is no direct contact to human breathing and not in direct exposure to the HVAC system. The number of occupants in the chamber is kept constant during the experiment, from the time the class began until the time the class ended. The IoT setup takes approximately fifteen minutes to stabilize, after which it constantly monitors the indoor air parameters at the sampling rate of 1 per minute.

3.1.2 Data Collection.: Data were collected at a sampling rate of 1 sample per minute, as the sampling interval must be small enough to capture subtle variations in indoor air pollutant concentrations from 9 AM in the morning to 5 PM in the evening, after which the classroom is closed. The observation data used in this work was recorded 6 days a week for a period of 14 months, from August 2018 to October 2019.

Figure 3 shows the daily variation in indoor temperature and relative humidity for the period of observation. The daily average value of temperature and relative humidity was determined from the samples recorded from 9 AM to 5 PM at a sampling interval of 1 minute. The mean, maximum and minimum values of temperature and relatively humidity were 18.4 C, 26.1 C, 21.35 C and 50%, 74%, 66.39% respectively. The daily average values of temperature and humidity have been used for the calculation of PPD.

The daily indoor concentration of CO_2 varied according to the plot shown in Figure 4. The maximum recorded value was 509 ppm, minimum was 419 ppm and the mean concentration was 453.58 ppm. The daily average CO_2 concentration is used for the calculation of ventilation rate.

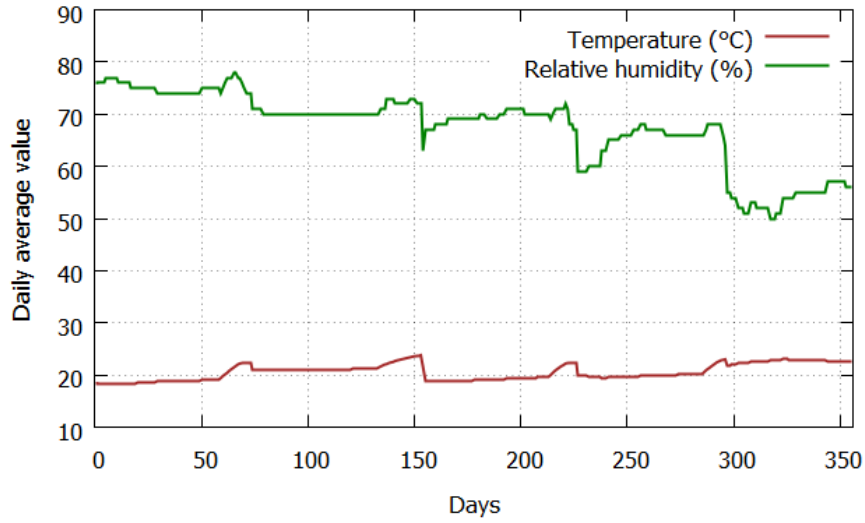


Fig.3: Temperature and relative humidity change with time

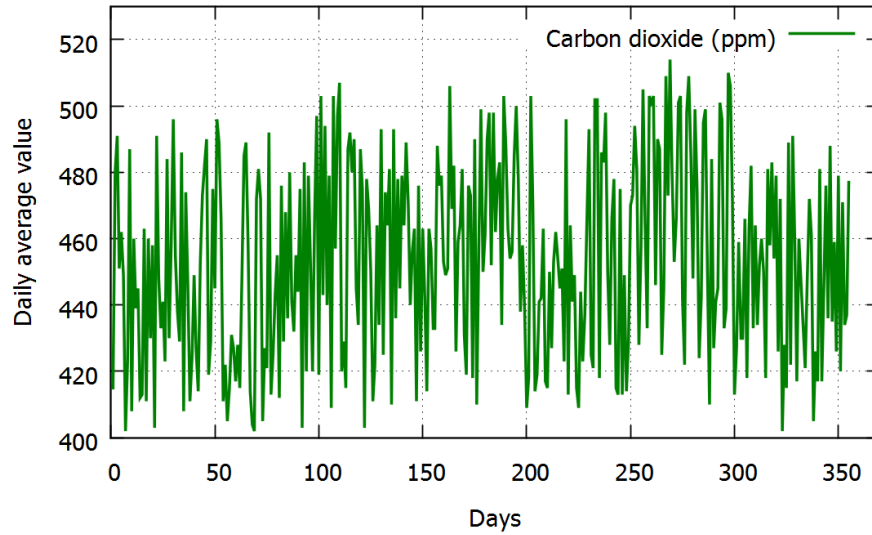


Fig.4: CO₂ build-up with time

The indoor pollutant CO doesn't show much variation in concentration over the period of observation with the maximum, minimum and mean values being 3.89 ppm, 1.01 ppm and 2.06 ppm respectively. But a large variation in the concentrations of $PM_{2.5}$ and PM_{10} is recorded with the maximum and minimum values being 301 g/m^3 , 17 g/m^3 and 365 g/m^3 , 22 g/m^3 respectively. The correlation between the concentrations of PM_{10} and $PM_{2.5}$ was calculated using Karl Pearson coefficient (Rastogi and Lohani, 2019):

$$\rho = \frac{n * \sum x_i \cdot y_i - \sum x_i \sum y_i}{\sqrt{n \sum x_i^2 - (\sum x_i)^2} \cdot \sqrt{n \sum y_i^2 - (\sum y_i)^2}} \tag{1}$$

where (x_i, y_i) is the i th pair observation value of $PM_{2.5}$ (x) and PM_{10} (y) respectively, $i = 1, 2, 3, \dots, n$.

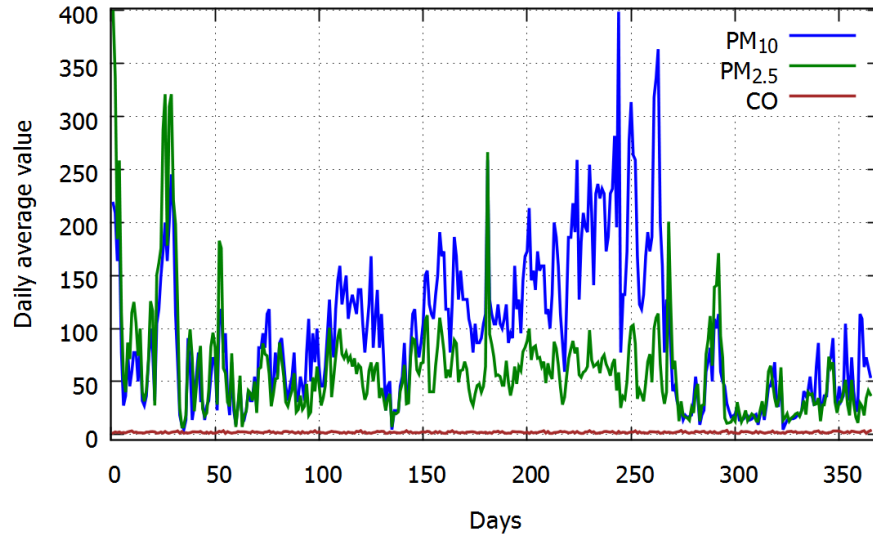


Fig.5: Graph depicting variation of indoor CO, $PM_{2.5}$ and PM_{10}

Karl Pearson correlation in this case came out to be 0.93, which showed a strong and positive correlation between the two pollutants.

4. PROPOSED INDOOR AIR QUALITY INDEX: STATE OF INDOOR AIR(SIA)

SIA is an indicator of the overall health of an enclosed place. It takes the air pollutant concentrations, ventilation and thermal comfort indicators into consideration to evaluate the state of indoor environment. Three prominent air pollutants $PM_{2.5}$, PM_{10} and CO are used to determine AQI of indoor space. The indoor CO_2 concentration is used in the calculation of ventilation rate. The temperature and relative humidity values in the room are used to evaluate the thermal comfort of occupants with the help of PPD. ANFIS combines the air pollution, ventilation and thermal comfort indicators AQI, VR and PPD to bring out the state of indoor air (SIA). SIA expresses the state of indoor air in terms of three levels - satisfactory, moderate and poor. The computation of AQI, VR and PPD, and the rules that ANFIS uses to determine SIA using these three parameters are described in detail in the following paragraphs.

4.1 Determination of Input Parameters for SIA Index

4.1.1 *Thermal Comfort.* The basic indices of thermal comfort are predicted mean vote (PMV) and predicted percentage dissatisfied (PPD). The main factors of discomfort are temperature and relative humidity. PMV is defined by the six most important thermal variables: human activities level, clothing insulation, mean radiant temperature, humidity, temperature and indoor air velocity. PMV is used as thermal comfort index that indicates mean thermal sensation vote on a standard scale for a large group of persons. ASHRAE defines the PMV scale with levels for thermal comfort: +3 (very hot) +2 (warm) +1 (slightly warm), 0 (neutral), -1 (cool); -2 (cold) -3 (very cold). On this scale, the PMV index is between -3 and +3. PMV is computed using the equation (Al horr. et al., 2016):

$$PMV = (0,303 e^{(-0,036M)+0,028}) * (M - W) - 3,05 * 10^{(-3)} * [5733 - 6,99(M - W) - p_a] - 0,42 * [(M - W) - 58,15] - 1,7 * 10^{(-5)} * M(34 - t_a) - 3,96 * 10^{(-8)} f_{cl} * h_c(t_{cl} - t_a) \quad (2)$$

where, M = Metabolic rate (met/m^2);
 W = external work (W/m^2), equal to 0 for driver or vehicle occupations;
 f_{cl} = ratio of clothed surface area of the body to that of nude body surface area;
 t_a = air temperature(C);
 p_a = water vapor pressure(Pa);
 h_c = convective heat transfer coefficient (W/m^2K);
 t_{cl} = surface temperature of clothing(C).

Assuming that all students (dressed in light cotton clothes) in the closed classroom are seated, W is taken as 0, M as $58 W/m^2$, p_a is calculated using the classroom ambient temperature, f_{cl} as 10, h_c is taken as 10.45 and t_{cl} is taken to be the same as t_a (Schiavon et al., 2017). Thermal dissatisfaction is represented as a percentage using PMV, to obtain the PPD index, which indirectly indicates the thermal comfort satisfaction. PPD is calculated using the equation below:

$$PPD = 100 - 95 * EXP(-0.03353 * PMV^4 - 0.2179 * PMV^2) \quad (3)$$

where, PPD Predicted Percentage Dissatisfied and PMV predicted mean vote. The relationship between PMV, PPD and thermal comfort is described in Table I.

Table I: ASHRAE Thermal Comfort Index (Yan et al. 2017)

PMV	Thermal Sensation	PPD	Category
+3	Very Hot	100	Satisfactory
+2	Warm	75	Moderate
+1	Slightly Warm	25	Poor
0	Neutral	5	Poor
-1	Cool	25	Poor
-2	Cold	75	Moderate
-3	Very Cold	100	Satisfactory

4.1.2 *Ventilation Rate.* The CO_2 concentration in an occupied indoor space indicates if the buildings air exchange balance is appropriate, i.e. if the optimal amount of outside air is mixing with the air inside the building. CO_2 is generated by human breathing. Each exhaled breath by an adult produces 35,000-50,000 ppm of CO_2 (Mendes et al., 2015). An elevated indoor CO_2 concentration is directly related to the number of occupants in the building, the buildings VR and the CO_2 level in the outside air. The time evolution of CO_2 concentration in any indoor space can be described using the mass balance equation (Cheng et al. 2012):

$$\left(\frac{dC_i(t)}{dt}\right) = -(C_{(i)}C_{(a)}) * \Lambda + \left(\frac{E}{V_R}\right) \quad (4)$$

where, C_i = tracer gas concentration in the indoor air, E = amount of tracer gas emitted per unit time, V_R = room volume, Λ = air change rate (ACR) and t = time. ACR or Λ is a measure of the volume of air that is added or removed from the classroom in unit time divided by the volume of the classroom.

The build-up of CO_2 is given by:

$$C(t) = C_0 exp(\Lambda t_i) \quad (5)$$

To obtain a linear relationship between tracer gas concentration $C_i(t)$ and the time t , the logarithm is taken on both sides:

$$\ln(C_i(t)) = \ln(C_0) + \Lambda * (t_i) \quad (6)$$

The above equation is used to calculate Λ using linear regression analysis. The build-up equation is then simplified as:

$$\ln(C(t)C_a) = \ln(C_o - C_a) + \Lambda * t \tag{7}$$

Where $C(t)$ is CO_2 concentration at time t (in hours), C_o and C_i are initial and background CO_2 concentrations respectively. VR can be determined using the value of Λ calculated in equation (4). VR can also be expressed as cubic feet per minute (CFM) (Lohani and Acharya, 2016):

$$cfm = \frac{\Lambda * Volumeofroom(cubicfeet)}{no.ofpersons * 60} \tag{8}$$

Here, the volume of the classroom under consideration is 49.51x39.50x9.58 feet and the occupancy of the classroom during experiment was fixed.

Table II: ASHRAE VR CATEGORY (RASTOGI ET AL., 2019)

Range	VR Category
0-12	Poor
12-15	Moderate
> 15	Satisfactory

4.1.3 *Indoor Air Quality Index.* AQI is a numerical scale used to communicate the current state indoor air quality with reference to the environment and human health. It briefs the occupants about how clean or polluted the air is, and the health effects related to the particular level of air quality. The higher the AQI value, the poorer the IAQ and the greater the health concern.

Table III: AQI CATEGORIES (RASTOGI ET AL., 2020)

Range	AQI Category
0-100	Satisfactory
101-200	Moderate
200-300	Poor

AQI is obtained by calculating the sub-indices of at-least three of the eight pollutants, PM_{10} , $PM_{2.5}$, NO_2 , SO_2 , CO , O_3 , NH_3 , and Pb . Sub-index of a pollutant is a linear function of the actual ambient concentration of the pollutant. The worst sub-index is the overall AQI. Conversion of multiple indoor air pollutants into a single AQI index is useful as it eliminated the need to build forecast models for each pollutant.

The sub-index for a pollutant is calculated using the following equation:

$$I_P = C_P - BP_{LO}X \frac{I_{HI} - I_{LO}}{BP_{HI} - BP_{LO}} \tag{9}$$

Where I_P is the index for pollutant p ,
 C_P is the rounded concentration of pollutant p ,
 BP_{HI} is the break-point that is greater than or equal to C_P ,
 BP_{LO} is the break-point that is less than or equal to C_P ,
 I_{HI} is the AQI value corresponding to BP_{HI} , and

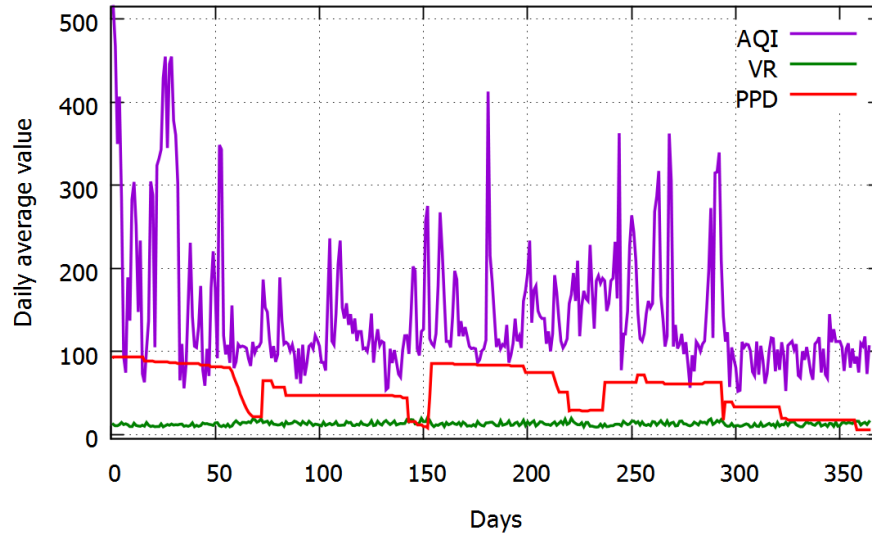


Fig. 6: Variation of daily average indoor PPD, VR and AQI

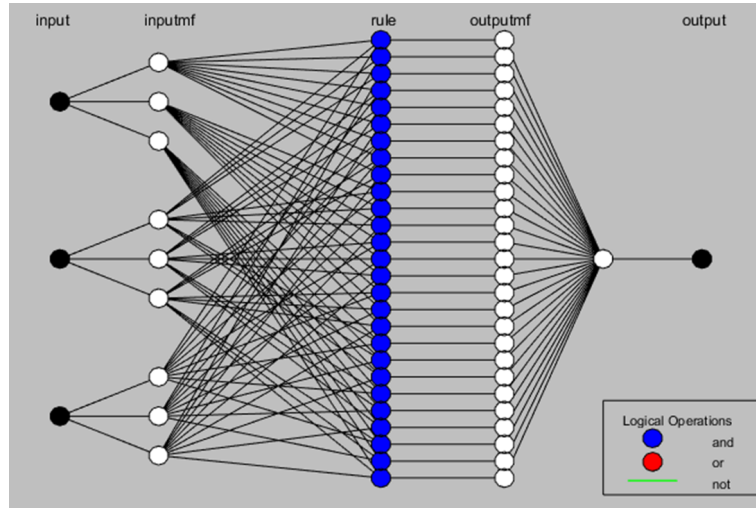
I_{LO} is the AQI value corresponding to BP_{LO} .

Figure 6 shows the relative variation of daily average indoor PPD (computed using relative humidity and temperature), VR (Computed using CO₂ concentration) and AQI (computed using daily average indoor $PM_{2.5}$, PM_{10} and CO concentrations) during the period from August, 2018 to October, 2019.

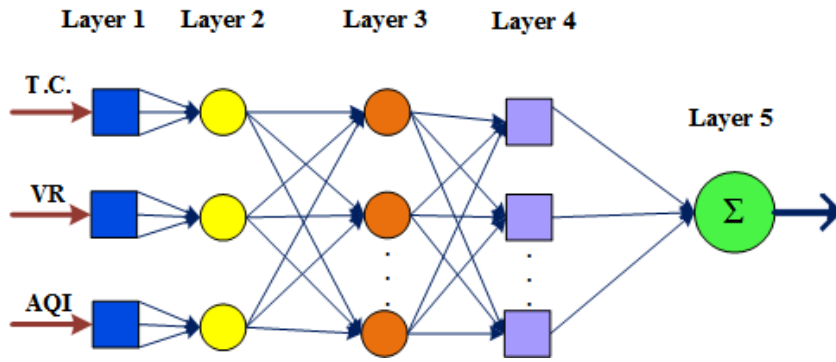
4.2 Calculation of Proposed SIA Index using Adaptive Neuro-Fuzzy Inference System

An adaptive neuro-fuzzy inference system (ANFIS) is a hybrid system composed of Fuzzy Inference System (FIS) with ANN features (J. et. al. 1993). ANFIS generates a stipulated input-output pair with membership function based on FIS. The FIS part performs various functions of converting the value to crisp fuzzy set and assigning the membership function, rules and decision unit. The mathematical model of the process is not needed and the process description with fuzzy rules emulates human thinking. Similar to FIS, the ANNs do not require a mathematical model of the process. In addition to FIS, ANNs offer learning/adapting capabilities (Prasad et al. 2016). The resultant neuro-fuzzy system is capable of learning new rules or membership functions, to optimize the existing ones. A multilayer feed-forward network which uses input to maps neural network learning algorithms and fuzzy reasoning into an output. The architecture of a typical ANFIS with two inputs, two rules and one output using the Takagi-Sugeno-Kang (TSK) model, where each input is assumed to have two membership functions (MFs) is shown in Figure 7.

Figure 8 depicts the flowchart to explain the working of the ANFIS system. The indoor air parameters are used as inputs to obtain the secondary variables PPD, VR and AQI in the first step. The secondary variables PPD, VR and AQI are used to express linguistic values in the form of fuzzy sets step 2, which are represented by the trapezoidal membership functions. The membership functions can be constructed with a range of the input and output variables classified into different number of linguistic values as satisfactory, medium and poor. The data sets are divided into two parts: training data-set and testing data-set of 80%-20% weightage. In order to generate FIS system, membership number and type were assigned to each input and output variables. For each input combinations, the model data set is trained and test. Rules are defined in step 3 according the variables and the logical AND is used in this case. Each function of the



(a) ANFIS structure generated by MATLAB



(b) Block diagram of ANFIS

Fig 7: Structure representation of ANFIS

variable has rules defined for it. The rule values are then added to form the proposed SIA index value which is obtained using summation function (Σ).

The working of each ANFIS layer is summarized and explained as follows. For layer 1, membership values for inputs can be generated by all nodes. The outputs of this layer are given by:

$$Q_{Ai}^1 = \mu_{Ai}(x), i = 1, 2, 3, N \tag{10}$$

$$Q_{Bi}^1 = \mu_{Bi}(y), i = 1, 2, 3, N \tag{11}$$

Where, x and y are crisp inputs, MFs characterized with low, medium, and high values of trapezoidal function. The current study utilized trapezoidal type MFs:

$$\mu_{Ai}(x) = \begin{cases} 0, & \text{if } (x < a) \text{ or } (x < b) \\ \frac{x-a}{b-a}, & \text{if } a \leq x \leq b \\ 1, & \text{if } b \leq x \leq c \\ \frac{d-x}{d-c}, & c \leq x \leq d \end{cases} \tag{12}$$

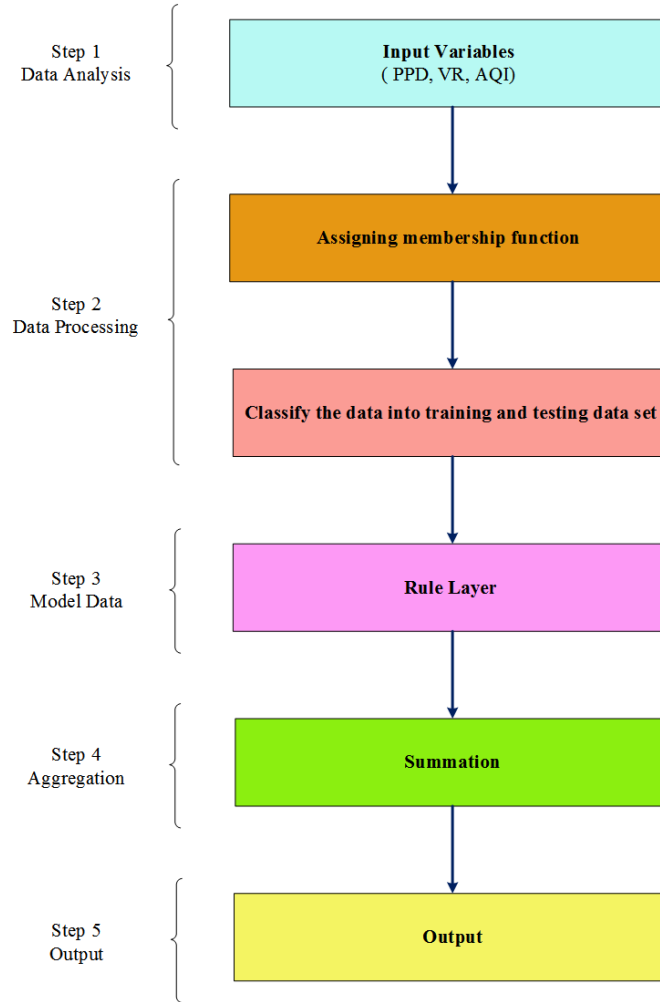


Fig 8: Flow chart explaining the functioning of the ANFIS system

$$\mu_{Bi}(y) = \begin{cases} 0, & \text{if } (y < a) \text{ or } (y < b) \\ \frac{y-a}{b-a}, & \text{if, } a \leq y \leq b \\ 1, & \text{if, } b \leq y \leq c \\ \frac{d-y}{d-c}, & c \leq y \leq d \end{cases} \quad (13)$$

For layer 2, the nodes act as multiplier and are fixed. The outputs of this layer are represented by:

$$Q_{ij}^2 = w_{ij} = \mu_{Ai}(x)\mu_{Bi}(y), i, j = 1, 2, 3, N \quad (14)$$

which represent the firing strength of each rule i.e. the degree to which the antecedent part of the rule is satisfied.

For layer 3, the nodes are also fixed, indicating that they play a normalization role in the network. The outputs which are called normalized firing strengths from this layer, can be represented

as follows:

$$\bar{W}_i = \frac{W_i}{(w_{11} + w_{12} + w_{21} + \dots + w_N)} \tag{15}$$

For layer 4, the parameters in this layer are referred to as consequent parameters. Each node is an adaptive node, and its output is simply the product of the normalized firing strength and a first-order polynomial. The outputs of this layer are given by:

$$O_1^4 = \bar{w}_i F_i = \bar{W}_i(px)(px + qy + r) \tag{16}$$

where p_{ij} , q_{ij} and r_{ij} are consequent parameters of the first-order polynomial. For layer 5, the single node which computes the summation of the entire incoming signal which is fixed node labeled:

$$Z = \sum (\bar{w}_i) f_i \tag{17}$$

SIA index is calculated by using the values of PPD, VR and AQI as inputs. PPD values between 0 and 100 are considered to be suitable for human comfort, ASHRAE recommends a VR of more than or equal to 15 cfm for classrooms (Kumar et. al., 2008) while AQI values between 0 and 300 are considered. The ANFIS controller has been considered for its flexibility, the little requirement of training data and its ability to model complex non-linear functions and more variables to combine together.

The rules that dictate SIA based on PPD, VR and AQI inputs are depicted in Figure 9.

Table IV: TABLE IV: RULES FOR CALCULATION OF PROPOSED SIA INDEX USING PPD, VR AND AQI

S. No.	Rule	SIA
1.	If $((70 \leq PPD \leq 100) \&\& (VR \geq 15) \&\& (AQI \leq 100))$	Satisfactory
2.	Else If $((25 \leq PPD \leq 70) \&\& (12 < VR < 15) \&\& (100 \leq AQI \leq 200))$	Moderate
3.	Else	Poor

The 3-D representation of SIA against AQI and VR, AQI and PPD, and VR and PPD is displayed in Figure 10. These graphs use different colors (as shown in Table IV) to indicate the three different states of indoor air, satisfactory, moderate and poor.

An AQI v/s PPD plot is shown in Figure 10(a). The state of indoor air improves with the decrease in the values of PPD and AQI, leading to satisfactory SIA. The red color in the graph represents a high value of AQI whereas a moderate value of thermal comfort is portrayed in yellow color. Figure 10(b) shows a 3-D plot between VR and PPD, which demonstrates that a higher value of VR and thermal comfort is synonymous with good state of indoor air. The plot indicates that the more the value, the more satisfactory is the state of indoor air. The 3D representation of AQI and VR in Figure 10(c) shows that the rise in AQI makes the state of indoor air poor. A combination of good VR of more than 15 cfm and satisfactory thermal comfort (PPD is more than 75) and AQI is less than 100 amounts to good SIA. PPD values between 50 and 75 or VR between 12 and 15 cfm and AQI between 100 and 200 signify moderate SIA. VR of less than 12 cfm or PPD values lesser than 25 and AQI is more than 200 are indicative of poor SIA.

5. FORECASTING SIA INDEX USING DISCRETE TIME MARKOV CHAIN MODEL

The indoor occupants are interested in the proportion of time for which the IAQ stays in a particular SIA state and the time after which an undesirable SIA will occur again. Therefore, Markov chains have been used to model the states of index formed from ANFIS. Markov chain is a stochastic model that is used to describe the sequence of possible SIA levels, where the probability of occurrence of each SIA level depends only on the state of the previous SIA. Hence, it satisfies the Markovian property (memoryless-ness). It means that no additional information

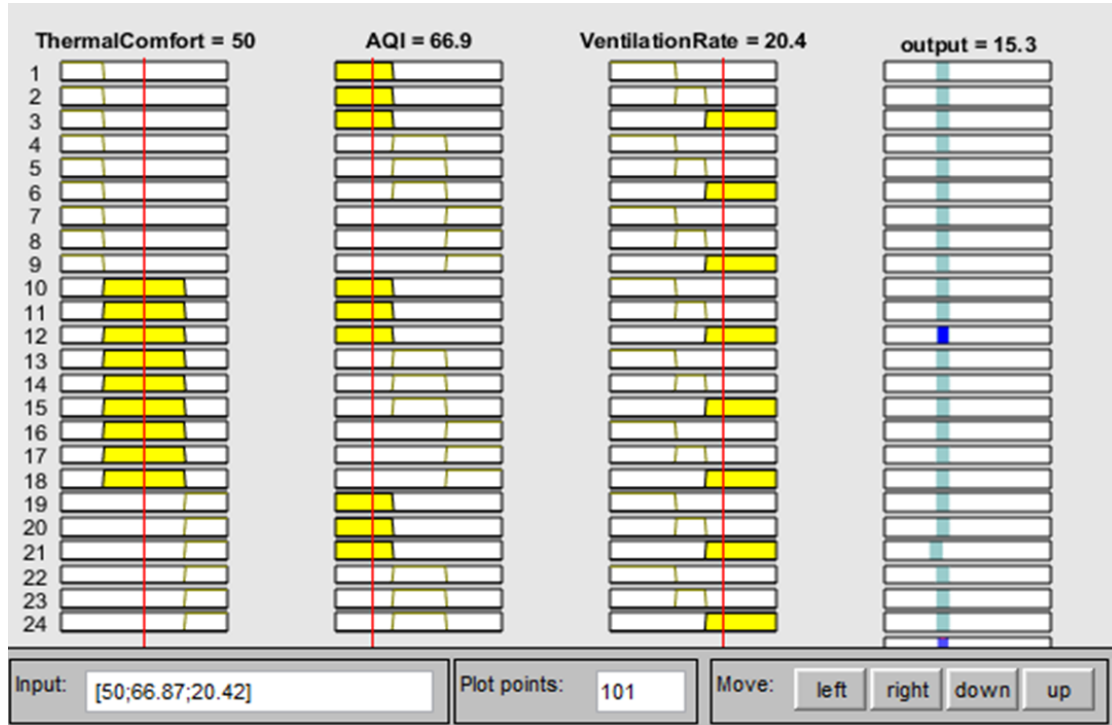


Fig.9. Rules of the ANFIS logic controller that dictate SIA output

of the past IAQ states is required if the current state of the stochastic process is known, to make best possible forecast of the future SIA state (Hoek and Elliott, 2012). This simplicity greatly reduces the number of parameters and hence Markov chains have been used in this work to model SIA states.

5.0.1 *Problem Formulation.* Let the SIA at time t be X_n , and at time $t + 1$ be X_{n+1} . According to the Markovian property, the future SIA, SIA at time $t + 1$ depends only on the present SIA, i.e. X_n . Let the sequence of events of SIA, $X = X_n; n=0,1, \dots, n$ be a random process which assumes the states $S= 1,2, \dots, m$. For this process to be a (DTMC), it must satisfy the property (Sericola et. al. 2013):

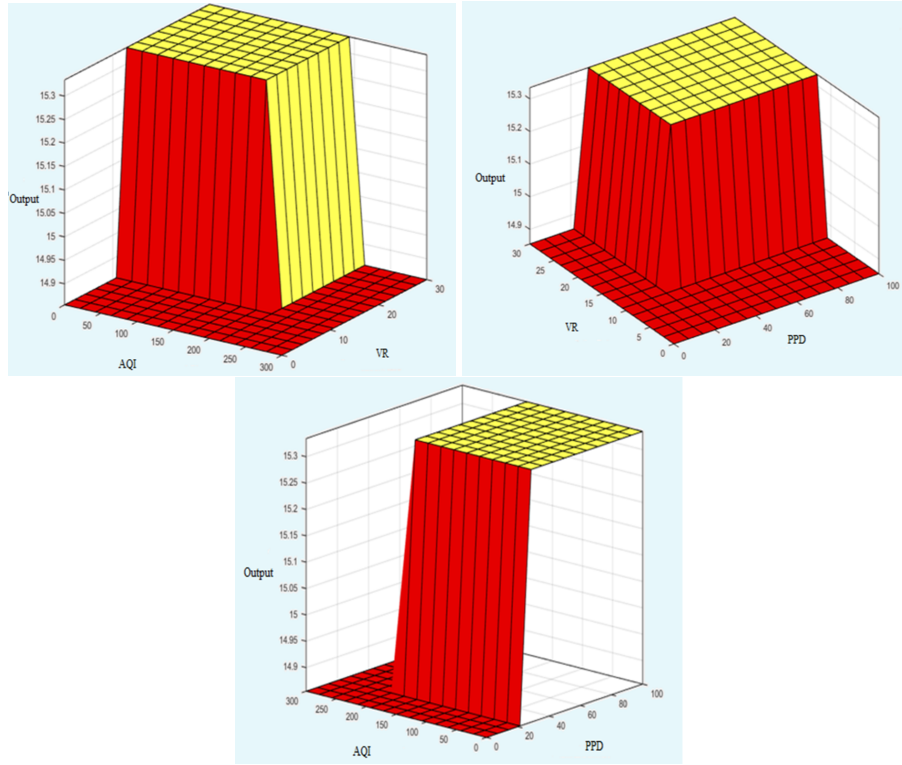
$$\begin{aligned}
 P(X_{n+1} = j | X_n = i, X_{n-1} = x_{n-1}, \dots, X_0 = x_0) \\
 = P(X_{n+1} = j | X_n = i)
 \end{aligned}
 \tag{18}$$

If the probabilities of transition between two states is independent of time, such a discrete time Markov chain (DTMC) and is represented by:

$$P(X_{n+1} = j | X_n = i) = P(X_1 = j | X_0 = i) = p_{ij}
 \tag{19}$$

Here, p_{ij} is the one-step transition probability from state i to state j . The one-step transition probability p_{ij} must satisfy the following properties:

$$\text{Property : } 1 - p_{ij} \geq 0, \text{ and}
 \tag{20}$$



(a) AQI vs VR, (b) VR vs PPD, (c) AQI vs PPD
 Fig.10. Output logic of the ANFIS logic controller

$$Property : 2 - \sum_{j=1}^m p_{ij} = 1 \tag{21}$$

Each place in the transition probability matrix represents the probability of transition from one SIA state to the another.

STATES	Poor	Moderate	Satisfactory
Poor	0.942	0.056	0.02
Moderate	0.926	0.052	0.22
Satisfactory	0.002	0.022	0.976

Each place in the transition probability matrix represents the probability of transition from one state to the another. Figure 11 shows the transition of the stochastic SIA process from one SIA state to another, according to the transition probability matrix.

To determine the proportion of time for which the stochastic process stays in a particular SIA state, the steady SIA states have been computed in the following sub-section.

5.0.2 *Steady AQI States.* Let the proportion of time for which the process stays in a particular AQI state i be denoted by π_i and is calculated using the following equations :

$$\pi_i = \sum_{k=1}^S \pi_k p_k, \text{ and} \tag{22}$$

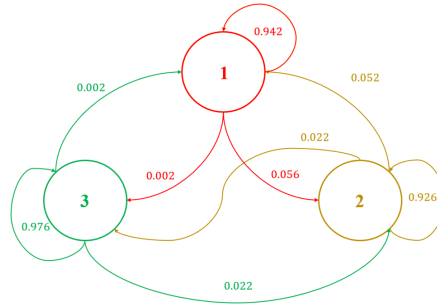


Fig. 11: SIA state transition diagram

$$\sum_{i \in S} \pi_k = 1 \tag{23}$$

$\forall i, j \in S$, and p_{ij} is the transition probability from state i to state j . A high value of π_i indicates that the probability of occurrence of state j is high. The steady state equations are obtained using the p_{ij} values from the transition probability matrix:

$$\pi_1 = 0.42\pi_1 + 0.052\pi_2 + 0.002\pi_3 \tag{24}$$

$$\pi_2 = 0.056\pi_1 + 0.926\pi_2 + 0.022\pi_3 \tag{25}$$

$$\pi_3 = 0.002\pi_1 + 0.022\pi_2 + 0.976\pi_3 \tag{26}$$

Solving the above linear equations for π_1, π_2 and π_3 , we get the results as :

$$\pi = \begin{bmatrix} \pi_1 \\ \pi_2 \\ \pi_3 \end{bmatrix} = \begin{bmatrix} 0.93 \\ 0.051 \\ 0.019 \end{bmatrix}$$

Equation (28) indicates that the prominent SIA state is 1 (represented by π_1). The classroom IAQ stays in moderate and satisfactory states (2 and 3) only 5.1% and 1.9% of the time respectively. According to the above equation, the SIA is predicted to be in poor state 93% of the time, which shows that the risk of exposure to harmful levels of pollution concentrations is very high.

5.0.3 . Calculation of Mean Return Period

Mean Return Period is the expected number of days required by the stochastic process to return to the same level i , if the Markov chain starts in i .

Mean return period predicted by the DTMC model for AQI level i is given as:

$$R_{ii} = \frac{1}{\pi_j} \tag{27}$$

This relation is used to predict the return period for each steady state:

$$R = \begin{bmatrix} 1.07 \\ 19.61 \\ 52.63 \end{bmatrix}$$

6. RESULTS AND DISCUSSION

The accuracy of the system is estimated by comparing the return periods of SIA levels predicted using the DTMC model with the actual values for the period of August, 2018 to October, 2019. The return period is the inferred time of recurrence of an event, such as exceedance of a certain value of SIA. The actual return period is the inverse of the probability of exceedance:

$$P\{(AQI) > (AQI_{TH})\} = \frac{\text{days on which AQI exceeds}}{\text{total no. of days}} \tag{28}$$

where, $P\{(AQI) > (AQI_{TH})\}$ is the probability of exceedance. The probability of exceedance of a SIA state is given as:

$$\text{Return Period} = \frac{1}{P\{(AQI) > (AQI_{TH})\}} \tag{29}$$

where, AQI_{TH} is the threshold value of an SIA state. The average absolute prediction error is %. The return period is best estimated for the indoor SIA state in Table V.

The error, percent error and absolute percent error are calculated using the formula below:

$$\text{Error} = \text{ActualRP} - \text{PredictedRP} \tag{30}$$

where, RP = return period

$$\%Error = \frac{(\text{ActualRP} - \text{PredictedRP})}{\text{ActualRP}} 100 \tag{31}$$

$$\%AbsoluteError = \frac{|(\text{ActualRP} - \text{PredictedRP})|}{\text{ActualRP}} 100 \tag{32}$$

Table V: Comparison Between Actual and Model Predicted Return Periods

State	Actual RP (days)	Predicted RP (days)	Error (days)	% Error
Poor	01.11	01.07	0.04	3.60
Moderate	18.01	19.61	-1.6	-1.88
Satisfactory	50.24	52.63	-12.39	-3.79

The prediction error for return periods of poor, moderate and satisfactory states is 3.26, -1.88 and 2.79% respectively. The DTMC models works best to forecast return periods for moderate SIA, followed by satisfactory and poor states. The low average absolute prediction error of 2.60% substantiates the use of DTMC model to forecast return periods of SIA levels. Hence, it is concluded that the DTMC model is highly accurate in forecasting states of indoor air.

7. CONCLUSION

An IoT system is developed for real time monitoring of indoor air pollutants and environmental parameters in a University classroom. It amalgamates the effects of indoor pollutant concentration, level of thermal comfort and the state of ventilation to represent the actual state of the indoor environment. The proposed SIA index is developed using ANFIS and is capable of describing the overall condition of environment inside the classroom. Thermal comfort is calculated with PPD using daily values of temperature and humidity, VR is calculated with the CO2 concentration, AQI is calculated using daily average concentrations of three pollutants (PM_{10} , $PM_{2.5}$, CO). The system then classifies indoor SIA into 3 states: Satisfactory, Moderate and Poor. Using annual SIA data, DTMC model is developed and used to predict return periods for

each of the 3 indoor SIA states. The predicted and actual return periods have been compared and the accuracy of the proposed model is found to be satisfactory with a low average absolute prediction error of 2.60%.

References

- AGEEV S., KOPCHAK Y., KOTENKO I. AND SAENKO I. 2015. Abnormal traffic detection in networks of the Internet of things based on fuzzy logical inference, *In Proceedings of XVIII International Conference on Soft Computing and Measurements (SCM), St. Petersburg*, 2015, 5-8 https://link.springer.com/chapter/10.1007%2F978-3-319-48829-5_8
- ASHRAE/ANSI STANDARD 62.1(2013). VENTILATION FOR ACCEPTABLE INDOOR AIR QUALITY. <http://www.myiaire.com/product-docs/ultraDRY/ASHRAE62.1.pdf>.
- BRODERICK ., BYRNE M., ARMSTRONG S., SHEAHAN J., COGGINS ANN MARIE. 2017. A pre and post evaluation of indoor air quality, ventilation, and thermal comfort in retrofitted co-operative social housing. *Building and Environment* 122, 126-133. <https://www.sciencedirect.com/science/article/abs/pii/S0360132317302007?via%3Dihub>
- BHATTACHARYA S., SRIDEVI S. AND PITCHIAH R. 2012. Indoor air quality monitoring using wireless sensor network. In Proceedings of Sixth International Conference on Sensing Technology, Kolkata *ICTS* 422-427. <https://ieeexplore.ieee.org/document/6461713>
- CHENG, YUANDA AND NIU, JIANLEI AND GAO, NAIPING. 2012 Thermal comfort models: A review and numerical investigation. *Building and Environment* 47. 1322. <http://www.sciencedirect.com/science/article/pii/S0360132311001508>
- DJAMILA H.. 2017. Indoor thermal comfort predictions: Selected issues and trends. *Renewable and Sustainable Energy Reviews* 74, 569-580. <https://ideas.repec.org/a/eee/rensus/v74y2017icp569-580.html>
- FANG, L., CLAUSEN, G. AND FANGER, P.O. 1998 Impact of Temperature and Humidity on the Perception of Indoor Air Quality. *Indoor Air* 8: 80-90. <https://onlinelibrary.wiley.com/doi/abs/10.1111/j.1600-0668.1998.t01-2-00003.x>
- HOEK J. AND ELLIOTT R. J. 2012. Asset Pricing Using Finite State Markov Chain Stochastic Discount Functions. *Stochastic Analysis and Applications* 30,5. <https://www.tandfonline.com/doi/full/10.1080/07362994.2012.704852>
- HORR A. Y., ARIF M., KATAFYGIOTOU M., MAZROEI A., KAUSHIK A., ELSARRAG E.. 2016. Impact of indoor environmental quality on occupant well-being and comfort: A review of the literature. *International Journal of Sustainable Built Environment*, 5, 1-11. <http://www.sciencedirect.com/science/article/pii/S2212609016300140>
- HORR A. Y., ARIF M., KATAFYGIOTOU M. , MAZROEI A. , SCHIAVON A. , S. , YANG, B. , DONNER, Y. , CHANG, V. W. AND NAZAROFF, W. W.. 2017. Thermal comfort, perceived air quality, and cognitive performance when personally controlled air movement is used by tropically acclimatized persons *Indoor Air* 27, 690-702. <https://onlinelibrary.wiley.com/doi/full/10.1111/ina.12352>
- JOHANSSON I., CARLSSON P., SANDBERG M., KUMLIN A. 2014. Emissions from concrete an indoor air quality issue? . *10th Nordic Symposium on Building Physics*, 330-337. https://www.nsb2014.se/wordpress/wp-content/uploads/2014/07/Building_Materials_and_Structures.pdf
- J. -. JANG R. . 1993. ANFIS: adaptive-network-based fuzzy inference system. *IEEE Transactions on Systems, Man, and Cybernetics*, 23, 665-685. <http://ieeexplore.ieee.org/stamp/stamp.jsp?tp=&arnumber=256541&isnumber=6499>
- KAUR J., KAUR K. 2017. A fuzzy approach for an IoT-based automated employee performance appraisal. *Computers, Materials and Continua*, 53, 23-36. <http://www.techscience.com/cmcc/v53n1/22847>
- KAUSHIK, ELSARRAG E. 2016. Impact of indoor environmental quality on occupant well-being and comfort: A review of the literature. *International Journal of Sustainable Built*

- Environment*, 5, 1-11.
- KO H. M., WEST G., SVETHAVENKATESH, KUMAR M..2018. Using dynamic time warping for online temporal fusion in multisensor systems. *Information Fusion*, 9, 370-388.<https://www.sciencedirect.com/science/article/abs/pii/S1566253506000674>
- KUMAR M. P. , LOKESH S., VARATHARAJAN R., X BABU C. G., PARTHASARATHY P.. 2018. Cloud and IoT based disease prediction and diagnosis system for healthcare using Fuzzy neural classifier. *Future Generation Computer Systems*, 86, 527-534.<https://www.sciencedirect.com/science/article/pii/S0167739X18303753>
- KIM J. Y., CHU C. H. AND SHIN S. M. 2014,ISSAQ: An Integrated Sensing Systems for Real-Time Indoor Air Quality Monitoring.*IEEE Sensors Journal*,14, 4230-4244.<http://ieeexplore.ieee.org/stamp/stamp.jsp?tp=&arnumber=6907986&isnumber=6933962>
- LOHANI D. AND ACHARYA D. 2016. SmartVent: A Context Aware IoT System to Measure Indoor Air Quality and Ventilation Rate. *In Proceedings of 17th IEEE International Conference on Mobile Data Management (MDM)*,Porto, 64-69.<https://ieeexplore.ieee.org/document/7551574>
- MEANA-LLORIN D., GARCA C. G., G-BUSTELO B. C. P., LOVELLE J. M. C., GARCIA-FERNANDEZ N. 2017.IoFClime: The fuzzy logic and the Internet of Things to control indoor temperature regarding the outdoor ambient conditions. *Future Generation Computer Systems*. 76, 275-284.
- MEANA-LLORIN D., GARCA C. G., G-BUSTELO B. C. P., LOVELLE J. M. C., GARCIA-FERNANDEZ N.. 2017. IoFClime: The fuzzy logic and the Internet of Things to control indoor temperature regarding the outdoor ambient conditions. *Future Generation Computer Systems*, 76, 275-284. <http://www.sciencedirect.com/science/article/pii/S0167739X16306598>
- MENDES A., BONASSI S., AGUIAR L., PEREIRA C., NEVES P., SILVA S., MENDES D., GUIMARES L., MORONI R., TEIXEIRA J. P. 2015 Indoor air quality and thermal comfort in elderly care centers. *Urban Climate*.14, 486-501. <https://www.sciencedirect.com/science/article/abs/pii/S2212095514000522>
- MEI J., XIA X..2017. Energy-efficient predictive control of indoor thermal comfort and air quality in a direct expansion air conditioning system. *Applied Energy*, 195, 439-452.<http://www.sciencedirect.com/science/article/pii/S0306261917303185>
- MOULIK S. AND MAJUMDAR S.. 2019. FallSense: An Automatic Fall Detection and Alarm Generation System in IoT-Enabled Environment. *IEEE Sensors Journal*, 19, 8452-8459.<http://ieeexplore.ieee.org/stamp/stamp.jsp?tp=&arnumber=8531728&isnumber=8825708>
- NORHIDAYAH A., CHIA-KUANG L., AZHAR M.K., NURULWAHIDA S. 2013. Indoor Air Quality and Sick Building Syndrome in Three Selected Buildings. *Procedia Engineering*, 53, 93-98.<https://www.sciencedirect.com/science/article/pii/S1877705813001331>
- PRASAD K., GORAI A. K., GOYAL P. 2016. Development of ANFIS models for air quality forecasting and input optimization for reducing the computational cost and time. *Atmospheric Environment*, 128, 246-262. <https://www.sciencedirect.com/science/article/abs/pii/S1352231016300073>
- RASTOGI K., BARTHWAL A. AND, LOHANI D. 2019. AQCI: An IoT Based Air Quality and Thermal Comfort Model using Fuzzy Inference. *In Proceedings of IEEE International Conference on Advanced Networks and Telecommunications Systems (ANTS)*, Goa, India.
- RASTOGI K. AND LOHANI D. 2019.IoT-based Occupancy Estimation Models for Indoor Non-Residential Environments, *IEEE 16thIndiaCouncilInternationalConference(INDICON)*, Rajkot, India, 1 – 4. : 10.1109/INDICON47234.2019.9030326.
- RASTOGI K., BARTHWAL A., LOHANI D. AND ACHARYA D. 2020. An IoT-based Discrete Time Markov Chain Model for Analysis and Prediction of Indoor Air Quality Index. *In*

- Proceedings of IEEE Sensors Applications Symposium (SAS), Kuala Lumpur, Malaysia.*
- SERICOLA B.2013. Markov Chains: Theory, Algorithms and Applications. In *ISTE Ltd and John Wiley and Sons Inc, London. John Wiley Sons, 9781848214934*, 410. <http://books.google.fr/books?id=tRdwAAAAQBAJ>
- STAZI F., NASPI F., ULPIANI G., PERNA C. D., 2017. INDOOR AIR QUALITY AND THERMAL COMFORT OPTIMIZATION IN CLASSROOMS DEVELOPING AN AUTOMATIC SYSTEM FOR WINDOWS OPENING AND CLOSING. *ENERGY AND BUILDINGS*, 139, 732-746. <https://www.sciencedirect.com/science/article/abs/pii/S0378778817300592>
- SPACHOS P. AND HATZINAKOS D.2016. Real-Time Indoor Carbon Dioxide Monitoring Through Cognitive Wireless Sensor Networks. *IEEE Sensors Journal*, 16, 506-514. <http://ieeexplore.ieee.org/stamp/stamp.jsp?tp=&arnumber=7270977&isnumber=7362261>
- SAAD S. M., SAAD M. R. A. , KAMARUDIN Y. M. A., ZAKARIA A. AND SHAKAFF M. Y. A.2013. Indoor air quality monitoring system using wireless sensor network (WSN) with web interface. In *Proceedings of International Conference on Electrical, Electronics and System Engineering (ICEESE), Kuala Lumpur, 2013*, 60-64. <http://ieeexplore.ieee.org/stamp/stamp.jsp?tp=&arnumber=6895043&isnumber=6895028>
- SCHIAVON, S. , YANG, B. , DONNER, Y. , CHANG, V. W. AND NAZAROFF, W. W. 2017. Thermal comfort, perceived air quality, and cognitive performance when personally controlled air movement is used by tropically acclimatized persons. *Indoor Air*, 27, 690-702. <https://doi.org/10.1111/ina.12352>. <http://www.sciencedirect.com/science/article/pii/S2212609016300140>
- UNITED STATES ENVIRONMENT PROTECTION AGENCY. 2018. Why Indoor Air Quality is Important to Schools. <https://www.epa.gov/iaq-schools/why-indoor-air-quality-important-schools>
- YU T., LIN C., CHEN C., LEE, LEE R., TSENG C., LIU S. 2013. Wireless sensor networks for indoor air quality monitoring. *Medical Engineering Physics*, 35, 231-235. <http://www.sciencedirect.com/science/article/pii/S1350453311002761>

Krati Rastogi is a Ph.D. Scholar in the Department of Computer Science and Engineering at Shiv Nadar University, India. Her research interests are in the areas of Wireless Sensors and Internet of Things.



Dr. Divya Lohani is currently serving as an Assistant Professor in the Department of Computer Science Engineering at Shiv Nadar University, India. She received her M.Tech (CSE) from Birla Institute of Technology, Mesra, Ranchi, India and her PhD from Indian Institute of Information Technology, Allahabad, India. Her research interests include Internet of Things, sensor networks, sensor data analytics, context aware computing, mobile computing and cybersecurity. She is a member of the Institute of Electrical and Electronics Engineers (IEEE).

